

Electron spectroscopic determinations of M and N core-hole lifetimes for the elements Nb—Te ($Z = 41 - 52$)

Nils Mårtensson and Ralf Nyholm

Institute of Physics, Uppsala University, Box 530, S-751 21 Uppsala, Sweden

(Received 2 March 1981)

Photoelectron spectroscopy has been used to determine M and N core-level widths for the elements Nb—Te ($Z = 41 - 52$). The analysis is based on direct comparisons of the lifetime contributions to different core levels. Absolute determinations are made for the narrow $3d$ levels. In the metals Nb—Rh ($Z = 41 - 45$) an $M_4M_5N_{45}$ Coster-Kronig decay channel is observed through a broadening of the $3d_{3/2}$ core-electron lines. The rate of this Coster-Kronig process is found to have its maximum for Ru and Rh. For Pd a much reduced, but still significant, broadening of the $3d_{3/2}$ level is detected. This observation is discussed in terms of itinerant versus quasiatomic contributions to the Coster-Kronig process. For $Z \geq 47$ (Ag) the Coster-Kronig channel is closed. For Nb—Rh the $M_4M_5N_{45}$ process can be used for absolute determinations of the $3d$ linewidths. In this connection also the properties of the $M_{45}N_{45}N_{45}$ Auger process are discussed. The accuracy of the present method makes it possible to investigate small differences between the $3p_{1/2}$ and $3p_{3/2}$ level widths. For several elements the unusual result is obtained that the $3p_{3/2}$ level is broader than the $3p_{1/2}$ level. This finding is in good agreement with theoretical predictions. The $4s$ and $4p$ spectra of the currently investigated elements are strongly influenced by configuration-interaction (CI) effects. However, the $4s$ line shapes are found to be quite normal for all the 5th-period elements. For $Z \leq 45$ (Rh) the $4p_{1/2}$ level is found to be broadened due to $N_2N_3N_{45}$ super-Coster-Kronig processes. For $Z \leq 46$ (Pd) the shape of the $4p_{3/2}$ core-electron lines can reasonably well be reproduced by broadened $3d_{5/2}$ line profiles. For $Z \geq 47$ (Ag) this can, however, not be achieved. This marks a transition into a region of Z values where CI effects become particularly important. The accuracy of the present method for determining core-level widths can be judged from a comparison between our analysis of the $4p$ levels and x-ray studies of the $M\zeta$ transition. The results indicate that core-level widths can be determined with an accuracy of about 0.2 eV even for fairly broad and asymmetric electron lines.

I. INTRODUCTION

One important piece of information which can be extracted from a photoelectron spectrum is the lifetime of a core hole. The lifetime broadening produces a Lorentzian contribution to the spectral line shape given by

$$A(E_k) = \frac{2A}{\pi} \frac{\Gamma}{4(E_k - E_n)^2 + \Gamma^2}, \quad (1)$$

where E_k is the kinetic energy of the outgoing electron, E_n the core-level binding energy, and A the intensity of the photoelectron line. The half-width Γ of the line can be expressed as a sum over transitions from the core-hole state to states in which the core hole is removed:

$$\Gamma = \sum_i \Gamma_i. \quad (2)$$

The relation between the Lorentzian broadening and the lifetime τ of the core hole is simply given by

$$\Gamma = \hbar/\tau, \quad (3)$$

where \hbar is Planck's constant divided by 2π . The observed spectrum will, however, also contain other contributions. One such contribution is due to the finite resolution of the spectrometer (see, e.g., Ref. 1). The spectrum will also be influenced by various shake-up processes. For instance, the core-electron lines in a metal will become asymmetric due to excitations of conduction-band electrons.²⁻⁶ Other contributions might be due to multiplet splitting, vibrational broadening, inelastic scattering, sample

charging, etc. A comprehensive review of the various broadening effects can be found in Ref. 6.

Accurate determinations of core-level widths are valuable in several respects. Firstly, it is important that these widths are known since they appear in all core-level spectroscopies. Secondly, the lifetime broadening plays an important role in the derivation of fluorescence yields.^{7,8} Furthermore, comparison with theoretical decay rates,^{9–11} is a sensitive test of the theoretical models. A summary of the present status of the field (theoretical and experimental) can be found in a recent work by Fugle and Alvarado.¹²

In this paper we will report accurate and consistently determined core-level widths for most of the 5th-period elements. Special effort has been made to separate the lifetime effects from other broadening mechanisms. The most favorable situation for a photoelectron spectroscopic determination of the natural linewidth is a closed-shell atom in the vapor phase. If the measurement is performed with a monochromatized x-ray source, the line profile can be approximated by a Voigt function, i.e., a convolution of a Lorentzian line profile with a Gaussian contribution due to the spectrometer broadening.¹ Owing to the different shapes of these contributions they can quite accurately be separated in a numerical fitting procedure.¹³ In the solid phase, however, this problem becomes considerably more difficult, especially for elements with pronounced core-line asymmetries. Even if there exist parametrizations which apply also to these situations, the number of fitting parameters becomes larger and the accuracy of the determined quantities will decrease.⁶

The present determination of core-level lifetimes relies on accurate comparisons of the lifetime contributions to different core levels. Absolute values are then determined for the $3d$ levels, which for most of the currently investigated elements show the narrowest electron lines. For the elements Nb–Rh ($Z = 41–45$) there is a strong $M_4M_5N_{45}$ Coster-Kronig decay of the $3d_{3/2}$ core holes. When this process is operating we can combine the measured broadening of the $3d_{3/2}$ level with the reduction in the M_4NN -to- M_5NN Auger intensity ratio in order to obtain absolute numbers for the $3d$ core-level widths.¹⁴ For Pd–Te ($Z = 46–52$) we must rely on more involved numerical fitting procedures where the core-line asymmetry is taken into account.^{2–6}

The paper will be organized as follows. After a brief account of the experimental details, Sec. II, we

describe our method for determining the core-level lifetimes in Sec. III. In Sec. IV the $M_4M_5N_{45}$ Coster-Kronig process is discussed, and in Sec. V the properties of the $M_{45}N_{45}N_{45}$ Auger process are studied. In Sec. VI we use our approach to determine the widths of the $3d_{3/2,5/2}$ levels. We then use these results to obtain accurate values also for the $3p_{1/2}$ and $3p_{3/2}$ levels, Sec. VII. In Sec. VIII the $4s$ levels are discussed and the $4p$ levels are analyzed in Sec. IX. Finally, in Sec. X we present a discussion and summary of our results.

II. EXPERIMENTAL

All the spectra in the present investigation have been recorded in the solid phase with a Hewlett-Packard 5950A ESCA (electron spectroscopy for chemical analysis) spectrometer. This spectrometer utilizes a monochromatized $AlK\alpha$ x-ray source for the excitation of the spectra. The spectrometer function has approximately a Gaussian shape with FWHM (full width at half maximum) close to 0.5 eV. To obtain maximum stability for the instrument, the standard HP power supplies, which are used to set the retardation potentials, were replaced by more accurate ones. In addition, the dispersion of the energy scan was carefully adjusted before the measurements.

All samples were mechanically cleaned *in situ*, at a pressure of 1 μ Pa, using a micromill with a rotating diamond edge. The pressure in the analyzing chamber was 100 nPa. It was not possible to keep the niobium sample entirely free from oxygen. However, no significant oxide contribution could be seen in the metal spectrum. The $3d$ spectra of all the currently studied elements are shown in a previous communication¹⁵ in which the M - and N -shell binding energies were reported.

III. METHOD FOR LIFETIME DETERMINATIONS

The determination of the lifetime contribution to a core-electron line recorded in the solid phase is in general a difficult task. The reason is that there are several other contributions to the measured spectrum which complicate the treatment. However, for a given element, very often most of these contributions will be the same for all core levels. Therefore, if one compares two or more core-electron lines from the same element, the difference in shape will mainly be due to differences in the core-hole life-

times. We know that the finite lifetime gives a Lorentzian contribution to the line shape. Therefore, in order to compare the lifetime broadenings of two core levels, we simply have to fold the narrower line with a Lorentzian function and vary the FWHM of this function until the shape of the broader line is reproduced. The required FWHM then directly gives the difference in lifetimes of the two core-hole states.

One complication which sometimes occurs in this kind of line-shape analysis is when two spin-orbit components are so close that they overlap. In this case, one must devise some accurate method to separate the two components. For this purpose we have used the deconvolution algorithm discussed in Ref. 16. This method relies on the single assumption that the line shapes of the two spin-orbit components are the same, except for a possible difference in the lifetime broadening. For a spin-orbit doublet this assumption can be expected to be particularly accurate. The algorithm makes it possible to separate two spin-orbit components, even in those cases where there is a large overlap between the lines. Figure 1 shows the result of this kind of separation for the Rh $3d$ spectrum. This does not represent a case where there is a large overlap between the two components. However, for further analysis it is important that the $3d_{5/2}$ single-line profile is accurately known over a region which is considerably larger than the $3d$ spin-orbit splitting. As can be seen from Fig. 1 the $3d_{3/2}$ line is significantly broader than the $3d_{5/2}$ line. The reason for the additional broadening of the Rh $3d_{3/2}$ line component is that there is an $M_4M_5N_{45}$ Coster-Kronig

decay channel, which considerably reduces the lifetime of the $3d_{3/2}$ hole state. These processes will be discussed in Sec. IV.

The low-binding-energy part of the spectrum is dominated by the contribution from the $3d_{5/2}$ line. Starting at a distance towards lower binding energies from the $3d_{5/2}$ line, at which the contribution also from this line has vanished, we can step through the spectrum and successively subtract a broadened (using a Lorentzian broadening function) replica of the $3d_{5/2}$ line (to represent the $3d_{3/2}$ line) at a distance Δ_{so} (the spin-orbit splitting) towards higher binding energies. The parameters of the procedure are thus the additional $3d_{3/2}$ (Coster-Kronig) broadening, the spin-orbit splitting, and the $3d_{3/2}$ -to- $3d_{5/2}$ intensity ratio, which are all varied until the resulting $3d_{5/2}$ single-line profile gets a physically reasonable line shape. It turns out that by inspection of the deconvoluted spectrum one can determine these parameters within quite narrow limits.¹⁶ This is so even in those cases where the $3d_{3/2}$ core-electron line is disturbed by a satellite from the $3d_{5/2}$ line as in Pd.¹⁷ For intensity ratios less than one, the algorithm will be stable and errors (due to statistical fluctuations or incorrectly chosen zero level for the starting point of the subtraction) will be damped as they are distributed through the spectrum by the subtraction procedure.

Above, we have outlined a method by which accurate relative determinations of core-level lifetimes can be made. For at least one level in each element we also have to make an absolute determination. For this purpose we have used the $3d$ spectra, which for most of the currently investigated elements show the narrowest lines. One possible way of determining the lifetime of a core level is to perform a numerical fit to the spectrum of some model line profile, which includes some expression for the core-line asymmetry. For the elements which have fairly symmetric line shapes, the Doniach-Šunjić profile² gives a good description of the spectra. For more asymmetric core lines it is known that this parametrization is not appropriate.^{5,6} However, by taking the band structure of the metal explicitly into account, it is possible to reproduce the core-line shapes also for the most asymmetric core lines.^{5,6} It has also been recognized^{5,6} that for these elements one can obtain a corresponding agreement with the parametrization by Mahan.³ In this case the two parameters (an asymmetry index and a cutoff parameter) are adjusted to obtain the best fit to the spectrum. The physical significance of the parameters determined in this way is, however, small.^{5,6}

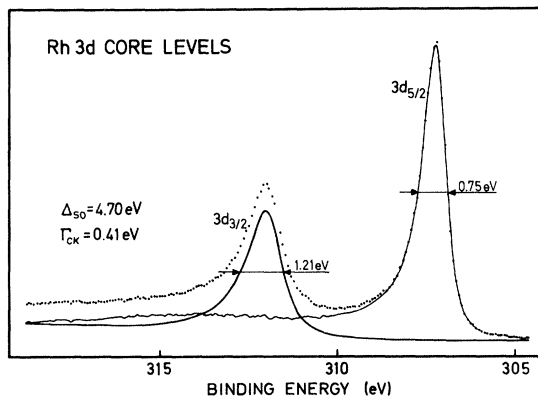


FIG. 1. The Rh $3d$ core-level spectrum resolved in its spin-orbit components.

If the $M_4M_5N_{45}$ Coster-Kronig process is allowed, the absolute $3d$ -level widths can be obtained without having to rely on any parametrization of the spectra. The magnitude of the Coster-Kronig broadening can be accurately determined by the deconvolution procedure outlined above. This broadening lies on top of the ordinary (mainly Auger) broadening of the $3d_{3/2}$ spin-orbit component, which in the following will be assumed to be the same as for the $3d_{5/2}$ level. The ratio between the Coster-Kronig decay rate Γ_{CK} and the Auger rate Γ_A determines what fraction of the initially produced $3d_{3/2}$ core holes will decay via ordinary Auger processes. Since one knows the ratio of initially populated $3d_{3/2}$ and $3d_{5/2}$ holes from the photoelectron intensity ratio, one can obtain the last piece of information from a study of the $M_{45}N_{45}N_{45}$ Auger spectrum. From the intensity ratio between the M_5 and the M_4 components of this spectrum, the ratio Γ_A/Γ_{CK} can be determined.

Before this can be done, however, one must know in more detail the nature of the $M_{45}N_{45}N_{45}$ Auger process. The Auger intensity, which disappears from the $M_4N_{45}N_{45}$ Auger spectrum due to the competing $M_4M_5N_{45}$ Coster-Kronig transition, must show up somewhere in the $M_5N_{45}N_{45}$ spectrum instead. The effect of the Coster-Kronig process is to transfer the M_4 hole state into a M_5N_{45} double-hole state. In the $M_5N_{45}N_{45}$ Auger region we will then observe the decay of this state into a $N_{45}N_{45}N_{45}$ triply ionized state. The first possibility is that this Auger vacancy satellite is shifted in energy relative to the $M_5N_{45}N_{45}$ Auger transition due to the presence of the additional N_{45} hole. This will be the case if the multiply ionized states involved have a localized character. This type of Auger satellites in metals have been identified in the analogous $L_{23}M_{45}M_{45}$ Auger spectra of metallic Cu and Zn.^{14,18–21} If the energy shift is so large that there is no contribution from the Auger satellite to the measured $M_5N_{45}N_{45}$ Auger intensity, one obtains the following relation for the Auger broadening Γ_A (Ref. 14):

$$\Gamma_A = \frac{3\Gamma_{CK}}{2I_A - 3} . \quad (4)$$

In this relation it is assumed that the statistical $3d_{5/2}$ -to- $3d_{3/2}$ photoionization cross-section ratio = 1.5 applies. The quantity

$$I_A = I(M_5N_{45}N_{45})/I(M_4N_{45}N_{45})$$

denotes the Auger intensity ratio without any contribution from the Auger satellite. However, as will

be discussed in the following section, the $M_4M_5N_{45}$ Coster-Kronig process is only allowed for elements where there is an itinerant character of the N_{45} holes in the final states of the $M_{45}N_{45}N_{45}$ Auger processes. If also the extra N_{45} hole created in the $M_4M_5N_{45}$ Coster-Kronig process is independent of the other holes, we expect no shift between the $M_4N_{45}N_{45}$ Auger transition and the $M_5N_{45}N_{45}N_{45}$ Auger satellite. In this case the satellite intensity will be indistinguishable from the ordinary $M_5N_{45}N_{45}$ Auger contribution and instead of Eq. (4) we will obtain

$$\Gamma_A = \frac{5\Gamma_{CK}}{2I_A - 3} . \quad (5)$$

The main assumption which has been made in Eqs. (4) and (5) is that the Auger decay rate Γ_A is the same for the $3d_{3/2}$ and $3d_{5/2}$ hole states. For I_A in relations (4) and (5) one should, in principle, use the ratio between the total number of Auger (and x-ray) decays of the $3d_{5/2}$ and $3d_{3/2}$ levels, respectively. However, by assuming that the partial Auger decay rates are the same for the two-hole states, I_A can be determined, e.g., from the $M_5N_{45}N_{45}$ -to- $M_4N_{45}N_{45}$ Auger intensity ratio. To arrive at Eq. (5) we also had to assume that the probability that the M_5N_{45} double-hole state decays via an $M_5N_{45}N_{45}$ Auger process is the same as for M_4 and M_5 single-hole states. Even if we expect these assumptions to be good, we now want to point out that the determined lifetime broadenings will not be very sensitive to small errors in the applied I_A values.

IV. THE $M_4M_5N_{45}$ COSTER-KRONIG PROCESS

The measured $3d$ photoelectron spectra, the valence-electron spectra, and the $M_{45}N_{45}N_{45}$ Auger spectra for the elements Mo–Cd are shown in Fig. 2. Looking at the $3d$ core-electron spectra, we first notice a marked difference between the elements $Z \leq 45$ (Rh) and $Z \geq 46$ (Pd). For the lighter elements the heights of the $3d_{3/2}$ components are considerably lower than suggested by the statistical $3d_{3/2}$ -to- $3d_{5/2}$ ratio of $\frac{2}{3}$. A closer inspection of the $3d$ spectra for Mo–Rh shows that the reduction in height is caused by a difference in widths for the two spin-orbit components. For the metals Mo–Rh the $3d_{3/2}$ hole state can decay into a $3d_{5/2}$ hole and an additional $4d$ -valence-band hole (i.e., an $M_4M_5N_{45}$ Coster-Kronig process), which will cause

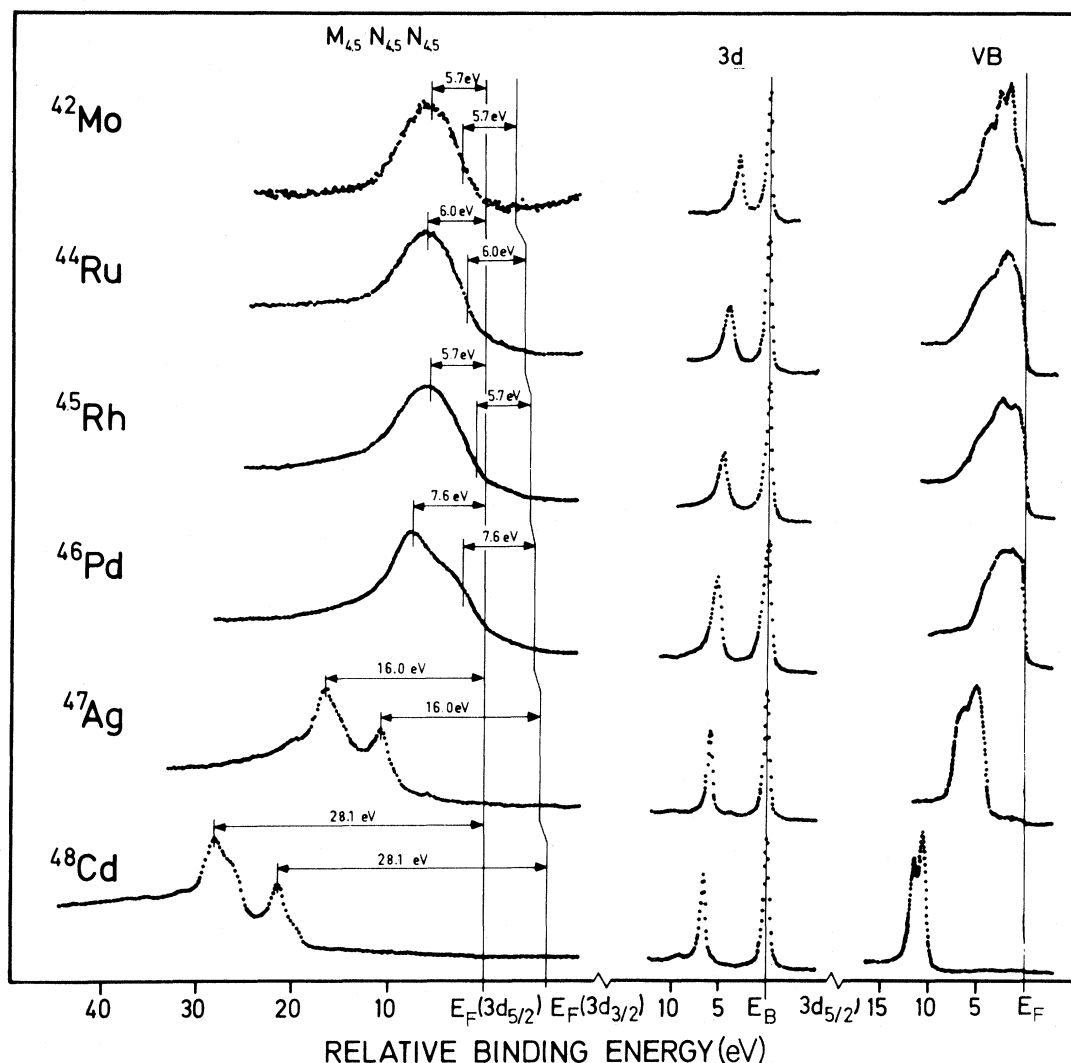


FIG. 2. $M_{45}N_{45}N_{45}$ Auger spectra, $3d$ -core-electron spectra, and valence-band spectra for the elements Mo to Cd.

an increased lifetime broadening of the $3d_{3/2}$ component.

Owing to the small $3d$ spin-orbit splitting for these elements, the excited Coster-Kronig electron will not, in general, have energy enough to leave the metal. We can therefore expect that this Coster-Kronig process will be forbidden for a nonmetallic sample. To test this assumption we have recorded the $3d$ spectrum from an insulating molybdenum compound, $(\text{NH}_4)_6\text{Mo}_7\text{O}_{24}$. Figure 3 shows the Mo $3d$ photoelectron spectra from this compound and from Mo metal. The expected change in the $3d$ spectrum does indeed occur and the $(\text{NH}_4)_6\text{Mo}_7\text{O}_{24}$ sample shows a normal $3d$ doublet with a $3d_{5/2}$ -to- $3d_{3/2}$ height ratio of $\frac{3}{2}$. Even if we take into ac-

count the fact that the resolution of our $(\text{NH}_4)_6\text{Mo}_7\text{O}_{24}$ spectrum is much lower than that of the metal spectrum and make a more careful comparison of the two spectra, the conclusion is that the Coster-Kronig broadening is considerably reduced in the compound.

For all the investigated metals we have used the deconvolution procedure described in the preceding section in order to analyze the $3d$ spin-orbit doublets. The results of this analysis are summarized in Table I. The spin-orbit splitting, the Coster-Kronig broadening, and in some cases also the $3d_{5/2}$ -to- $3d_{3/2}$ intensity ratio have been free parameters in this treatment. However, it is found that it is rather difficult to separate the effect of a small change in

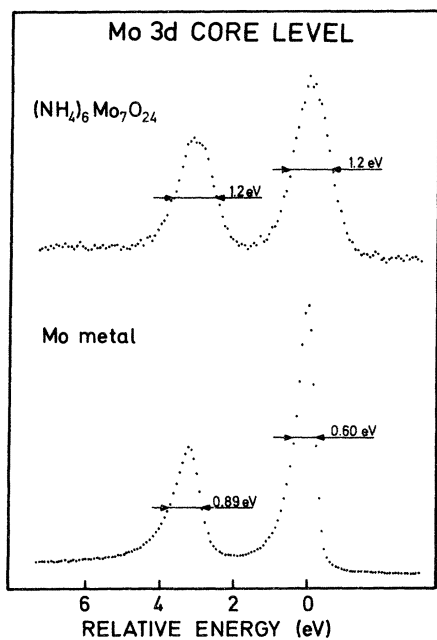


FIG. 3. The Mo 3d spectrum from ammonium molybdate, $(\text{NH}_4)_6\text{Mo}_7\text{O}_{24}$, and metallic molybdenum. The Coster-Kronig channel responsible for the broadening of the $3d_{3/2}$ level in the metal is closed in the salt.

the Coster-Kronig broadening and a small change in the intensity ratio on the resulting single-line profile. Therefore, in those cases where there is a broadening of the $3d_{3/2}$ component, we have chosen to use the statistical $3d_{3/2}$ -to- $3d_{5/2}$ intensity ratio. For Ag—Te there is no Coster-Kronig broadening of the $3d_{3/2}$ level and for these elements the deconvolutions yield intensity ratios of 0.67—0.70. These values are also in close agreement with the calculations by Scofield,²² which for all the currently investigated elements predict a ratio of 0.69. Thus the assumption of a statistical intensity ratio for Nb—Pd seems to be justified. A choice of 0.69 instead would give only slightly larger values for the determined Coster-Kronig broadenings.

From Table I we can observe that the Coster-Kronig rate increases with atomic number up to Ru and Rh, where it reaches its largest value. Between Rh and Pd there is an abrupt change in the broadening. For $Z \geq 47$ (Ag) the $3d$ spin-orbit components are found to be equally broad. For Pd, however, there is a small but significant Coster-Kronig broadening of 0.04 eV. The quenching of the $M_4M_5N_{45}$ Coster-Kronig decay channel around Pd in the Periodic Table marks a change over from

TABLE I. Results from deconvolutions of the $3d$ photoelectron spectra and the $M_{45}N_{45}N_{45}$ Auger spectra. The Coster-Kronig broadening Γ_{CK} , and the spin-orbit splitting Δ_{so} were in all cases treated as free parameters in the deconvolutions. The intensity $I(3d_{3/2})$ was fixed at 0.67 when analyzing the elements Nb—Pd, whereas for Ag—Te it was treated as a free parameter. The Auger intensity $I(M_4N_{45}N_{45})$ was estimated through a deconvolution of the $M_{45}N_{45}N_{45}$ Auger spectrum. The Auger rate Γ_A is obtained from $I(M_4N_{45}N_{45})$ and Γ_{CK} [see Eqs. (4) and (5)]. The maximum errors are given in parentheses.

Element	Γ_{CK} (eV)	Δ_{so} (eV)	$I(3d_{3/2})^a$	$I(M_4N_{45}N_{45})^b$	Γ_A (eV)
Nb	0.17(4)	2.73(2)	0.67	0.1(1)	0.05(5)
Mo	0.30(3)	3.13(2)	0.67	0.10(5)	0.09(5)
Ru	0.43(4)	4.14(2)	0.67	0.15(5)	0.21(10)
Rh	0.41(4)	4.70(2)	0.67	0.15(5)	0.20(10)
Pd	0.04(3)	5.27(2)	0.67		
Ag	0	5.99(1)	0.67(2)		
Cd	0	6.74(2)	0.67(2)		
In	0	7.54(2)	0.70(2)		
Sn	0	8.42(1)	0.68(2)		
Sb	0	9.37(1)	0.68(2)		
Te	0	10.38(2)	0.69(2)		

^aIntensity relative to $3d_{5/2}$.

^bIntensity relative to $M_5N_{45}N_{45}$.

a region in which the M_5N_{45} Auger final state has a delocalized character to a region for which this state becomes localized. The localization of the Coster-Kronig final state for Pd has been previously discussed.^{17,23} In Ref. 17 it was demonstrated that for Pd a localized M_5N_{45} state is more bound than the M_4 single-hole state. The detection of a small Coster-Kronig broadening for Pd thus indicates that there is a vestige of a bandlike behavior in the $M_4M_5N_{45}$ transition. (For a discussion of the relation between the quasiatomic and bandlike part of an Auger spectrum for narrow d -band materials, see Refs. 24 and 25.) By comparison with Ru and Rh, we could expect a broadening of about 0.4 eV if the Coster-Kronig final state were bandlike also for Pd. The bandlike part of the Coster-Kronig decay thus seems to be reduced by about a factor of 10.

V. $M_{45}N_{45}N_{45}$ AUGER SPECTRA

In Sec. III it was shown how the $M_4M_5N_{45}$ Coster-Kronig process can be used to determine the $3d$ -level widths. This requires that the $M_{45}N_{45}N_{45}$ Auger spectra also are analyzed. Figure 2 shows the $M_{45}N_{45}N_{45}$ spectra for the elements Mo—Cd ($Z = 42-48$).²⁶ The spectra are plotted in such a way that the energy scale shows the total energy of

the two-hole states relative to the Fermi level. As for the $3d$ photoelectron spectra, we observe a significant change in the shape of the spectra between Rh and Pd. In Ref. 17 it was shown that the Rh spectrum can be well reproduced by a self-convolution of the metal valence-band spectrum. The Pd spectrum can instead be described in terms of the multiplets of a totally screened local $4d^8$ configuration.^{17,23} In Table II we present the kinetic energies of the most pronounced $M_5N_{45}N_{45}$ structure for each of the elements Nb—Te. In this table we also give the energies of the two-hole final states relative to the Fermi level. These energies are compared to the energy which is required in order to create two independent $4d$ holes. This comparison again demonstrates that the picture of independent $4d$ holes applies to Nb—Rh but not to the rest of the elements. For Pd—Te, where the Auger spectra show atomiclike behavior, the energies in Table II correspond to the $4d^8^1G_4$ multiplet. In the spectra that show atomiclike Auger final states, there might also be a bandlike contribution.^{24,25} A particularly intense bandlike spectrum is found in palladium.²⁷ This can be compared to the observation made for the $M_4M_5N_{45}$ Coster-Kronig process in Pd, where also a small bandlike decay channel was found besides the dominating atomiclike contribution. For

TABLE II. Measured kinetic energies (eV) and related values for the $M_5N_{45}N_{45}$ Auger line in the elements Nb to Te. The maximum errors are given in parentheses.

Element	$E_k(M_5N_{45}N_{45}, ^1G_4)$			$N_{45}N_{45}$ Auger final-state energy ^a	
	This work	Ref. 28	Ref. 29	Expt.	$E_{VB} * V_B^b$
Nb	199.0(5)			3.2	~ 3
Mo	222.2(5)			5.7	5.0
Ru	274.0(5)			6.0	5.4
Rh	301.5(5)			5.8	5.1
Pd	327.5(4)			7.6	4.0
Ag	352.2(3)	351.9(3)		16.0	11.1
Cd	377.0(3)	376.7(2)		28.1	22.2
In	403.1(3)	402.6(3)	402.85(15)	40.8	34.3
Sn	429.1(3)	428.9(2)	428.85(15)	55.8	48.7
Sb	455.3(3)		454.90(15)	72.9	65.1
Te	481.9(3)		481.79(15)	91.0	82.1

^aThe effective two-hole Coulomb interaction (U_{eff}), introduced by Sawatzky (Ref. 25), is given by the difference between the energies in the last two columns of the table.

^bFor the elements Nb to Pd these values correspond to the maximum of the self-convolution of the valence band. For the elements Ag to Te the values are given by twice the weighted mean binding energy of the $4d$ levels.

the elements Ag—Te we can compare our measured Auger energies to values from the literature.^{28,29} As can be seen the agreement is in all cases very good.

There is another pronounced difference between the $M_{45}N_{45}N_{45}$ Auger spectra for the elements with $Z \leq 45$ (Rh) and $Z \geq 46$ (Pd). For Pd—Cd two peaks, corresponding to the M_4 and M_5 components, can clearly be seen. The intensity ratio between the two components is close to the statistical ratio of $\frac{2}{3}$. However, for the lighter elements the M_4 component is hardly discernable. Its intensity has for these elements dropped down to a value close to $\frac{1}{10}$. This reduction of the $M_4N_{45}N_{45}$ Auger intensity is due to the $M_4M_5N_{45}$ Coster-Kronig process, which offers an additional decay channel for the $3d_{3/2}$ hole state.

VI. $3d$ CORE-LEVEL WIDTHS

For most of the currently investigated elements, the $3d$ spectra show the narrowest core-electron lines. We will therefore use these spectra for making absolute determinations of the core-level widths. For the elements Nb—Rh the $M_4M_5N_{45}$ Coster-Kronig process is operating, and the $3d_{5/2}$ -level widths can be obtained through Eqs. (4) and (5). To determine the Auger intensity ratios which enter into these equations we have used the same type of deconvolution procedure as that, for the $3d$ core levels. The only difference is that in order to obtain a numerically stable procedure, one has to start the subtraction from the low kinetic energy side of the spectrum. The intensity ratios so obtained for Nb—Rh are given in Table I. Since the Auger spectra for these elements show a typical bandlike behavior, we have accordingly used Eq. (5) to obtain values for Γ_A . The determined Auger broadenings are displayed in the last column of Table I. In this determination the dominating source of error is the uncertainty in the Auger intensity ratios. We can never expect to separate the two Auger components with the same high accuracy as for the $3d$ components in the photoelectron spectra. This is so since the Auger spectra are quite broad compared to the spin-orbit splitting, the intensity ratios are small, and the spectra are, furthermore, quite featureless. However, the errors in the determined Auger intensity ratios should not be larger than 5% in units of the $M_5N_{45}N_{45}$ Auger intensity. Even with this relatively large error the $3d_{5/2}$ level widths can be expected to be accurate to about 0.1 eV.

TABLE III. Results from fitting a Doniach-Šunjić line profile to the measured $3d_{5/2}$ spectra from Ag to Te. 2γ is the natural linewidth and α is the asymmetry parameter. The maximum errors are given in parentheses.

Element	2γ (eV)	α
Ag	0.29(5)	0.08(2)
Cd	0.33(5)	0.09(2)
In	0.33(5)	0.10(2)
Sn	0.39(5)	0.11(2)
Sb	0.48(5)	0.09(2)
Te	0.61(5)	0.11(2)

For the remaining elements, Pd—Te, we must rely on various numerical fitting procedures. For Ag—Te, which show fairly symmetric core-electron lines, the $3d$ spectra have been fitted by the Doniach-Šunjić profile.² The parameters (lifetime broadenings and asymmetry indices) which come out of the analysis are summarized in Table III. In all cases a Gaussian spectrometer function of 0.5 eV has been assumed. For the more asymmetric Pd core lines the Doniach-Šunjić parametrization will not be very accurate. For this element we have therefore used the value which Citrin and Wertheim⁶ obtained in their more detailed line-shape analysis, see Sec. III. They reported a Lorentzian broadening of 0.22 eV for the Pd $3d_{5/2}$ level.³⁰

In Fig. 4 we have plotted the $3d_{3/2}$ and $3d_{5/2}$ core-level widths for the elements Nb—Xe. The values are also summarized in columns 4 and 5 of Table IV. The value for Xe in Fig. 4 has been taken from a line-shape analysis of the $3d$ photoelectron spectrum recorded in the gas phase.^{31,32} From Fig. 4 one observes that quite consistent values have been obtained for the $3d_{5/2}$ level over the whole range of Z values, although different methods have been used for different elements. Taking the degree of consistency as a measure of the errors in the determinations, it seems that the values in Fig. 4 are determined with an accuracy close to 0.1 eV. This high accuracy is obtained in spite of the fact that the lifetime broadening in many cases gives only a very small contribution to the total width. The only exception from the smooth trend is the value for Te, which seems to be somewhat too high. The probable cause for this is that the resolution of the spec-

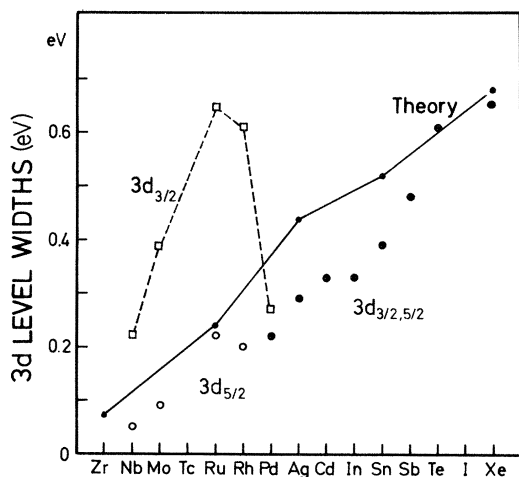


FIG. 4. Experimental level widths for the $3d_{3/2}$ and the $3d_{5/2}$ levels. Open circles ($3d_{5/2}$) are derived from the $M_5N_{45}N_{45}$ -to- $M_4N_{45}N_{45}$ Auger intensity ratios and the $3d_{3/2}$ Coster-Kronig broadenings. Open squares ($3d_{3/2}$) are taken as the sum of the $3d_{5/2}$ level widths and the $3d_{3/2}$ Coster-Kronig broadenings. Filled circles ($3d_{3/2}$ and $3d_{5/2}$) are results from fitting a Doniac-Šunjić (Ref. 2) line profile to the $3d_{5/2}$ spectra. The value for Pd is taken from Ref. 6. Experimental values for Xe have also been included (Refs. 31 and 32). Included are also theoretical values from Refs. 9 and 10.

trum was somewhat poorer for the Te sample than for the other elements. However, one cannot exclude the possibility that there are inherent broadening mechanisms for Te, which are not taken into account in the present analysis.

TABLE IV. Summary of the measured natural level widths for M and N shells in the elements Nb to Te. Maximum errors are given in parentheses.

Element	$3p_{1/2}$	$3p_{3/2}$	$3d_{3/2}$	$3d_{5/2}$	$4s$	$4p_{1/2}$	$4p_{3/2}$
Nb	2.08(13)	2.12(13)	0.22(9)	0.05(5)	2.8(3)	1.5(3)	0.99(15)
Mo	2.28(13)	2.20(13)	0.39(8)	0.09(5)	b	2.2(3)	1.57(15)
Ru	2.48(18)	2.44(18)	0.64(14)	0.21(10)	3.2(5) ^c	3.3(3)	2.51(20)
Rh	2.54(18)	2.54(18)	0.61(14)	0.20(10)	3.4(5) ^c	4.2(3)	3.40(20)
Pd	2.52(13)	2.68(13)	0.26(8)	0.22 ^a	4.2(5) ^c	4.7(4) ^d	4.7(4) ^d
Ag	2.63(13)	2.79(13)	0.29(5)	0.29(5)	5.4(3)		
Cd	2.83(13)	3.14(15)	0.33(5)	0.33(5)	4.8(3)		
In	2.99(15)	3.30(15)	0.33(5)	0.33(5)	4.8(3)		
Sn	3.20(15)	3.36(20)	0.39(5)	0.39(5)	3.8(3)		
Sb	3.37(20)	3.76(20)	0.48(5)	0.48(5)	3.3(3)		
Te	3.58(23)	4.05(23)	0.61(8)	0.61(8)	3.0(3)		

^aFrom Ref. 6.

^bOverlapping with a plasmon loss from the $4p$ levels.

^cSomewhat uncertain values due to traces of Au and/or Pt in the samples.

^dThe $4p$ spectrum was deconvoluted using a spin-orbit splitting of 4.0 eV.

For Cd we can compare our value with a study made by Aksela *et al.* in the gas phase using Auger electron spectroscopy.^{33,34} From this measurement a width for the $M_{45}N_{45}N_{45}$ lines of 0.32 eV was found. Since we can expect that the final state in the Auger process will not contribute significantly to the total Auger linewidth, the agreement with our fitted value is very good.

For comparison we have included in Fig. 4 the theoretical $3d_{5/2}$ widths from McGuire.^{9,10} Thereby, we notice first that the experimental trend is well reproduced by the calculations. Furthermore, the discussion above suggests that even the small difference between the experimental and the theoretical values (≤ 0.15 eV) is significant.

VII. $3p$ CORE-LEVEL WIDTHS

We will now use the determined $3d_{5/2}$ line broadenings to derive widths for other core levels. In a previous investigation of the photoelectron spectrum of Xe, performed in the vapor phase,³¹ an unusual result was obtained: The $3p_{3/2}$ level is broader than the $3p_{1/2}$ level. The same result has been obtained theoretically by McGuire.^{9,10} For lower Z values his calculations indicate that the situation is reversed, i.e., that the $3p_{1/2}$ level is somewhat broader. The calculations predict that the change occurs around Nb or Mo. We will now investigate if it is possible to obtain experimental lifetime broadenings that are sufficiently accurate to judge if the theoretical behavior agrees with ex-

periment. This requires that differences of the order of 0.1 eV have to be detected on levels which are several eV broad. At first sight this might seem quite optimistic since spectra have to be analyzed which have quite different shapes in terms of core-line asymmetries, satellite structures, etc.

In order to determine the $3p$ natural linewidths we have used the method outlined in Sec. III. The different steps of the treatment are demonstrated for the Pd $3p_{3/2}$ level in Fig. 5. This element is chosen

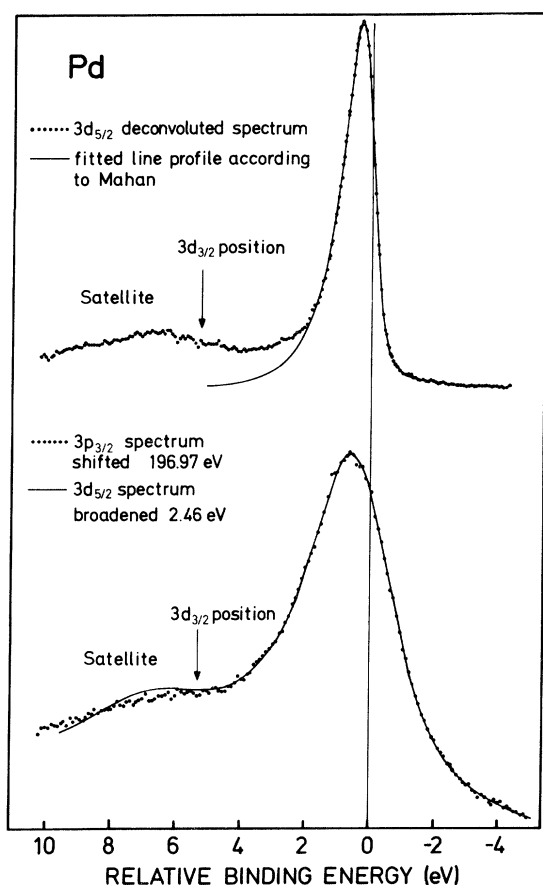


FIG. 5. The present method of deriving natural level widths is demonstrated for the Pd $3p_{3/2}$ spectrum. The upper part of the figure shows the $3d_{5/2}$ spectrum after subtraction of the $3d_{3/2}$ component. In the lower part of the figure a broadened $3d_{5/2}$ profile is compared to the $3p_{3/2}$ spectrum. The Lorentzian broadening required to reproduce the $3p_{3/2}$ spectrum directly gives the difference in level widths. The broad satellite structure in the $3p_{3/2}$ spectrum is also well described by the broadened $3d_{5/2}$ line. In the upper part a fitted theoretical line profile [Mahan's solution (Ref. 3)] is compared to the $3d_{5/2}$ spectrum.

since the analysis involves two major complications. Firstly, the Pd $3d$ levels show large asymmetries and secondly, the Pd core lines are accompanied by intense shake-up structures. The upper part of Fig. 5 shows the $3d_{5/2}$ line profile after subtraction of the $3d_{3/2}$ component.¹⁶ The position of the $3d_{3/2}$ electron line is marked, and as can be seen this line coincides with the $3d_{5/2}$ satellite. However, by the deconvolution procedure, these two contributions can be accurately separated. Figure 5 also shows how a model line profile, based on the parametrization by Mahan,³ can be fitted to the $3d_{5/2}$ spectrum. As was mentioned in Sec. III, this fit closely resembles the line profile, which was obtained by Wertheim and co-workers,^{5,6} by taking the Pd band structure into account. As can be seen, the $3d_{5/2}$ spectrum is reproduced within an energy region of about 1.5 eV from the peak position. This is sufficient for estimating the Lorentzian contribution to the narrow Pd $3d_{5/2}$ level. However, for a broader line, like the $3p_{3/2}$ line, a corresponding analysis seems somewhat meaningless. Instead, the lower part of Fig. 5 demonstrates how the $3p_{3/2}$ line profile, including the satellite, can be almost exactly reproduced by a broadened $3d_{5/2}$ single-line profile. Together with the previously determined $3d_{5/2}$ lifetime, the required broadening can be used to calculate the $3p_{3/2}$ -level width. Since the complete core-level spectrum can be used in this comparison, the derived widths can be expected to be determined with a high accuracy.³⁵

As a further application of the present treatment, we can compare in a very direct way the intensities of the shake-up satellites from different levels. It has been reported that the Pd $3p$ satellite lines are much more intense than the corresponding $3d$ satellites.³⁶ However, Fig. 5 demonstrates that the $3p$ and $3d$ satellites have almost identical intensities relative to their parent lines.

In Fig. 6 we show the $3p$ linewidths which have been obtained in this way. From Fig. 6 we can conclude that consistent values of core-level lifetimes can be derived from photoelectron spectra, and that complications due to core-line asymmetries and interacting shake-up structures can be mastered. The accuracy of the currently determined values is estimated to be better than 0.2 eV. In Fig. 6 we have also plotted the theoretical results by McGuire.^{9,10} As can be seen, the theoretical and the experimental trends are the same. The experiments indicate that the $3p_{3/2}$ width exceeds the $3p_{1/2}$ width for $Z \geq 46$ (Pd). For $Z \leq 45$ (Rh), we can only conclude that the two linewidths

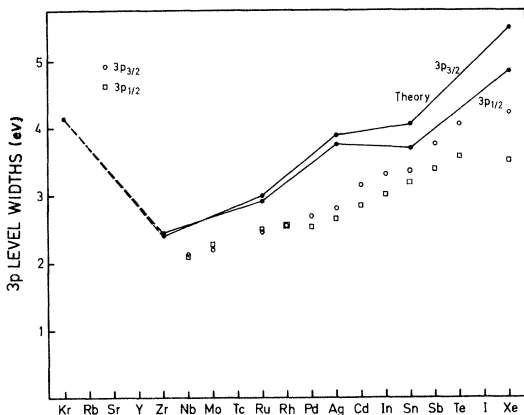


FIG. 6. Experimental level widths for the $3p_{1/2}$ and the $3p_{3/2}$ levels together with theoretical values from Refs. 9 and 10. Experimental values for Xe have also been included (Refs. 31 and 32).

are very similar. As a general result we find that the absolute values of the lifetime widths are somewhat overestimated by the calculations, whereas the differences between the $3p_{1/2}$ and $3p_{3/2}$ widths are very well reproduced by the calculations. The large decrease of the theoretical $3p$ level widths, somewhere between Kr and Zr, is due to the closing of the $M_{23}M_{45}M_{45}$ super-Coster-Kronig decay channel. However, Svensson *et al.*³¹ have previously shown that this channel is essentially closed already for Kr.

VIII. $4s$ CORE-LEVEL WIDTHS

The $4s$ -core-electron spectra for a large number of elements around Xe in the Periodic Table are known to show strong deviations from predictions based on the independent-particle model.³⁷ For instance, using Δ SCF (self-consistent-field) calculations for the Xe $4s$ level, a binding energy is obtained which is 10 eV too high.³⁷ This indicates that the $4s$ spectrum is strongly influenced by CI (configuration—interaction) effects. However, applying the procedure which was outlined in Sec. III, it is found that in all the currently investigated elements the $4s$ spectra can be obtained from a Lorentzian broadening of the $3d_{5/2}$ single-line profile.

The determined $4s$ -level widths are summarized in Table IV. These values show that the $4s$ broadening has a pronounced maximum for Ag in this series of elements. The decay of the $4s$ hole

states is expected to be dominated by $N_1N_{23}N_{45}$ super-Coster-Kronig processes.¹¹ It can be noted that these super-Coster-Kronig electrons have their maximum kinetic energies close to the elements for which the broadest $4s$ levels are found.³⁸

IX. $4p$ LINE BROADENINGS

A particularly strong breakdown of the one-electron picture is found for the $4p$ levels in the elements around Xe in the Periodic Table.^{31,37} For instance, the Xe $4p_{1/2}$ line is completely absent in the photoelectron spectrum. Neither does the $4p_{3/2}$ hole exist as an elementary excitation. The main spectral strength of these ionizations becomes spread out over a large energy range instead.³⁷ We will now investigate if, for any of the currently investigated elements, the $4p$ core lines have the same shape as the other lines in the spectrum, i.e., to find out in which elements Eq. (1) is valid for the $4p$ ionization.

As a first step we must separate the closely spaced $4p_{1/2}$ and $4p_{3/2}$ spin-orbit components. In a previous communication it was demonstrated that there is a $N_2N_3N_{45}$ super-Coster-Kronig broadening of the $4p_{1/2}$ levels for the elements $Z \leq 45$ (Rh).¹⁶ Owing to the large widths of the $4p$ lines, no numerical values were derived for the broadenings in Ru and Rh. However, if we compare the obtained

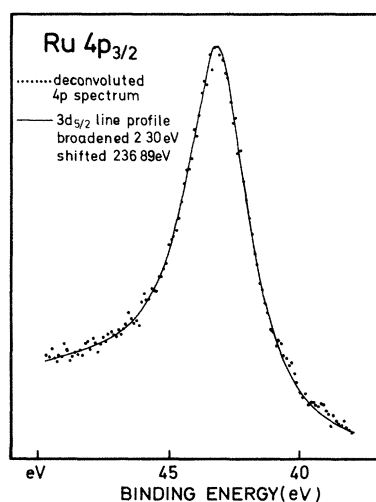


FIG. 7. The line shape of the Ru $4p_{3/2}$ spectrum is compared to a broadened $3d_{5/2}$ line profile. The $4p_{1/2}$ and $3d_{3/2}$ lines have been removed by a deconvolution procedure.

$4p_{3/2}$ single-line profile for each deconvolution of the $4p$ spectra with a broadened $3d_{5/2}$ spectrum, the sensitivity of the deconvolution procedure can be considerably increased. Figure 7 demonstrates the agreement which is obtained between a broadened $3d_{5/2}$ line and a deconvoluted $4p$ spectrum for Ru. The $4p_{3/2}$ line profile is obtained with a $4p_{1/2}$ broadening of 0.8 eV. For Rh a super-Coster-Kronig broadening of about 0.8 eV is also found in this way. For Pd a deconvolution can be made with the same width for the two components. The absence of the super-Coster-Kronig decay channel for Pd is consistent with the results for the $M_4M_5N_{45}$ Coster-Kronig process, see Sec. IV. However, the large widths of the Pd $4p$ lines make this analysis very uncertain. A more reliable result is that the obtained $4p_{3/2}$ single-line profile can be fairly well reproduced by a broadened $3d_{5/2}$ spectrum.

For Ag—Te it is, however, impossible to reproduce the spectrum with two spin-orbit components that are broadened replicas of some other core-electron line. For these elements the analysis indicates a smearing out of the spectra towards higher binding energies. As it seems relevant to discuss a $4p$ -level width [i.e., application of Eq. (1)] for $Z \leq 46$ (Pd), we have given the obtained $4p$ -level widths for these elements in Table IV.

An independent method for obtaining information about core-level lifetimes is by means of x-ray emission spectroscopy. For the $4d$ transition elements the $M\zeta$ transition ($3d_{5/2}-4p_{3/2}$) has a low energy which makes it possible to study the x-ray line shapes at high resolution. The shape of such an x-ray transition will be essentially Lorentzian with a FWHM, which is the sum of the lifetimes of the initial and final hole states. Dannhäuser and Wiech³⁹

TABLE V. FWHM of the $M\zeta$ transition from Nb to Rh obtained by adding the $3d_{5/2}$ and the $4p_{3/2}$ level widths. The values from Ref. 39 were measured with x-ray emission spectroscopy. Maximum errors are given in parentheses.

Element	$\Gamma(M\zeta)$ (eV)	
	This work	Ref. 39
Nb	1.04(20)	1.21
Mo	1.66(20)	1.56
Ru	2.72(30)	2.49
Rh	3.60(30)	3.77

have studied the $M\zeta$ transitions in Nb—Rh ($Z = 41-45$) with a grating spectrometer. In Table V their obtained $M\zeta$ widths are compared to the sum of the $3d_{5/2}$ and $4p_{3/2}$ widths from this work. The differences between these two sets of values are only of the order of 0.2 eV. In this comparison one has to remember that the x-ray measurements have been made at a resolution of about 0.6 eV, and that the x-ray line shape is slightly distorted by other transition. Furthermore, the presently determined widths are obtained as a sum of two core-level widths, i.e., the error in both the $3d_{5/2}$ and the $4p_{3/2}$ widths will contribute.

X. DISCUSSION AND SUMMARY

M and N core-level widths for most of the 5th-period elements have been determined. It is demonstrated that from metallic photoelectron spectra one can determine accurate core-level widths. The problems which are caused by the core-line asymmetries and interacting satellite lines can be handled. The internal consistency of the results suggests that the accuracy of the determined level widths is of the order of 0.1–0.2 eV, even for fairly broad electron lines. Comparison with literature data on the $M\zeta$ —x-ray transition also indicates the same accuracy. This is a considerable improvement, compared to previous determinations of core-level lifetimes.

In the metals Nb—Rh ($Z = 41-45$) an $M_4M_5N_{45}$ broadening of the $3d_{3/2}$ level is observed. The extent of this broadening is largest for Ru and Rh. For Pd a small but significant broadening of the $3d_{3/2}$ level is observed. This broadening indicates a small fraction of a bandlike behavior of the $M_4M_5N_{45}$ Coster-Kronig process, in addition to the dominating quasiautomatic character. The $4p_{1/2}$ levels for Nb—Rh are broadened relative to the $4p_{3/2}$ levels. This broadening is due to the $N_2N_3N_{45}$ super-Coster-Kronig process, and its rate is found to be about twice that of the $M_4M_5N_{45}$ process.

The determined $3d$ and $3p$ widths have been compared to calculations. The widths of the $3d_{5/2}$ lines are found to be only slightly overestimated by McGuire's^{9,10} calculations. The $3p$ -level widths are also somewhat overestimated. For $Z \geq 46$ (Pd) it is found that the $3p_{3/2}$ level is broader than the $3p_{1/2}$ level. This property of the spectrum is very well reproduced by the calculations and can be attributed to a difference in the rate of the $M_{23}M_{45}N$ Coster-Kronig processes for a $3p_{1/2}$ and a $3p_{3/2}$ hole state.

The $4s$ and $4p$ spectra are known to be consider-

ably influenced by CI effects,^{31,37} especially for the later 5th-period elements. In this work we find that, in spite of these CI effects, the 4s line shapes can be well reproduced by broadened $3d_{5/2}$ spectra. The same is observed for the 4p spectra from

Nb—Pd. However, for the elements Ag—Te the 4p line shapes have changed considerably, which shows that the CI effects become particularly important in these spectra.

- ¹U. Gelius, E. Basilier, S. Svensson, T. Bergmark, and K. Siegbahn, *J. Electron Spectrosc. Relat. Phenom.* **2**, 405 (1974).
- ²S. Doniach and M. Šunjić, *J. Phys. C* **3**, 285 (1970).
- ³G. D. Mahan, *Phys. Rev. B* **11**, 4814 (1975).
- ⁴P. H. Citrin, G. K. Wertheim, and Y. Baer, *Phys. Rev. B* **16**, 4256 (1977).
- ⁵G. K. Wertheim and L. R. Walker, *J. Phys. F* **6**, 2297 (1976).
- ⁶G. K. Wertheim and P. H. Citrin, in *Photoemission in Solids I*, Vol. 26 of *Topics in Applied Physics*, edited by M. Cardona and L. Ley (Springer, Berlin, 1978).
- ⁷M. O. Krause, *J. Phys. Chem. Ref. Data* **8**, 307 (1979).
- ⁸M. O. Krause and J. H. Oliver, *J. Phys. Chem. Ref. Data* **8**, 329 (1979).
- ⁹E. J. McGuire, *Phys. Rev. A* **5**, 1043 (1972).
- ¹⁰E. J. McGuire, *Phys. Rev. A* **5**, 1052 (1972).
- ¹¹E. J. McGuire, *Phys. Rev. A* **9**, 1840 (1974).
- ¹²J. C. Fuggle and S. F. Alvarado, *Phys. Rev. A* **22**, 1615 (1980).
- ¹³G. K. Wertheim, M. A. Butler, K. W. West, and D. N. E. Buchanan, *Rev. Sci. Instrum.* **45**, 1369 (1974).
- ¹⁴E. Antonides, E. C. Janse, and G. A. Sawatzky, *Phys. Rev. B* **15**, 4596 (1977).
- ¹⁵R. Nyholm and N. Mårtensson, *J. Phys. C* **13**, L279 (1980).
- ¹⁶R. Nyholm and N. Mårtensson, *Chem. Phys. Lett.* **74**, 337 (1980).
- ¹⁷N. Mårtensson, R. Nyholm, and B. Johansson, *Phys. Rev. Lett.* **45**, 754 (1980).
- ¹⁸H. H. Madden, D. M. Zehner, and J. R. Noonan, *Phys. Rev. B* **17**, 3074 (1978).
- ¹⁹E. Antonides and G. A. Sawatzky, *J. Phys. C* **9**, L547 (1976).
- ²⁰P. Weightman and P. T. Andrews, *J. Phys. C* **12**, 943 (1979).
- ²¹H. W. Haak, G. A. Sawatzky, and T. D. Thomas, *Phys. Rev. Lett.* **41**, 1825 (1978).
- ²²J. H. Scofield, *J. Electron Spectrosc. Relat. Phenom.* **8**, 129 (1976).
- ²³N. Mårtensson and B. Johansson, *Phys. Rev. Lett.* **45**, 482 (1980).
- ²⁴M. Cini, *Solid State Commun.* **20**, 605 (1976).
- ²⁵G. A. Sawatzky, *Phys. Rev. Lett.* **39**, 504 (1977).
- ²⁶Since the HP spectrometer is based on the method of dispersion compensation (Ref. 1) the Auger spectra have not been obtained with optimal resolution. To obtain maximum intensity in the photoelectron spectra, a relatively large portion of the AlK α peak is used for the excitation, but the dispersion of the x rays is compensated for by the electron optics. However, when secondary processes are studied this design leads instead to a broadening of the spectra.
- ²⁷N. Mårtensson, R. Nyholm, H. Calén, J. Hedman, and B. Johansson *Phys. Rev. B*, in press.
- ²⁸A. C. Parry-Jones, P. Weightman, and P. T. Andrews, *J. Phys. C* **12**, 1587 (1979).
- ²⁹M. Pessa, A. Vuoristo, M. Vulli, S. Aksela, J. Väyrynen, T. Rantala, and H. Aksela, *Phys. Rev. B* **20**, 3115 (1979).
- ³⁰For a dilute Cu_{1-x}Pd_x alloy the Pd 3d core-level asymmetry is much reduced (Ref. 17) and we can apply the Doniach-Šunjić profile. From such an analysis we obtain a width of 0.27 eV, i.e., reasonably close to the value obtained by Wertheim and Citrin (Ref. 6).
- ³¹S. Svensson, N. Mårtensson, E. Basilier, P. Å. Malmquist, U. Gelius, and K. Siegbahn, *Phys. Scr.* **14**, 141 (1976).
- ³²The values for Xe have been slightly changed compared to the ones given in Ref. 31. To obtain a comparable accuracy for Xe, as for the other elements, we have reanalyzed the spectra according to the method outlined in Sec. III. We have used the 5p_{3/2} line as a reference and we have simply assumed that the 5p_{3/2} level has a negligible lifetime width compared to the deeper levels. We then obtain for the 4d levels a width of 0.18 eV, for the 3d levels 0.64 eV, and for the 3p_{3/2} level we find a width of 4.2 eV. To obtain the 3p_{1/2} width (3.5 eV) we have subtracted the 3p_{3/2}-3p_{1/2} width difference of 0.7 eV which was found in Ref. 31.
- ³³H. Aksela and S. Aksela, *J. Phys. B* **7**, 1262 (1974).
- ³⁴S. Aksela, H. Aksela, M. Vuontisjärvi, J. Väyrynen, and E. Lähteenkorva, *J. Electron Spectrosc. Relat. Phenom.* **11**, 137 (1977).
- ³⁵As another result of the present analysis, accurate core-level positions can also be obtained. In this way corrections can be made for the shifts of the peak positions, away from the ground-state core-hole energies, which are caused by the core-line asymmetry and by interacting satellite lines. This application will be further discussed elsewhere.
- ³⁶K. Berndt, U. Marx, and O. Brummer, *Phys. Status Solidi B* **94**, 541 (1979).
- ³⁷G. Wendin and M. Ohno, *Phys. Scr.* **14**, 148 (1976).
- ³⁸For the elements with $Z \leq 45$ (Rh) the kinetic energies will increase with increasing Z values due to an increasing 4s binding energy. For the elements with Z

≥ 46 (Pd) the $4p$ $4d$ hole state will be localized and the final-state energy will increase faster than the $4s$ initial-hole-state energy.

³⁹G. Dannhäuser and G. Wiech, Z. Phys. 244, 429 (1971).